

Wound healing after excision of subcutaneous tumors treated with near-infrared photoimmunotherapy

Adrian Rosenberg | Fuyuki Inagaki  | Takuya Kato | Ryuhei Okada | Hiroaki Wakiyama | Aki Furusawa | Peter L. Choyke | Hisataka Kobayashi 

Molecular Imaging Program, Center for Cancer Research, National Cancer Institute, National Institutes of Health, Bethesda, MD, USA

Correspondence

Hisataka Kobayashi, National Institutes of Health, Building 10, Room B3B69, MSC 1088, 10 Center Drive, Bethesda, MD 20892, USA.

Email: kobayash@mail.nih.gov

Funding information

National Cancer Institute, Grant/Award Number: ZIA BC 011513; National Center for Global Health and Medicine Research Institute; NIH Medical Research Scholars Program

Abstract

Near-infrared photoimmunotherapy (NIR-PIT) is a novel cancer therapy that employs a combination of infrared light and tumor-targeted monoclonal antibody-photoabsorber conjugates to cause both direct tumor necrosis and immunogenic cell death. NIR-PIT may have potential in the perioperative setting before surgery, and therefore it is important to know the effect of NIR-PIT on wound healing. Fifty mice were implanted with subcutaneous xenografts of N87 human gastric cancer cells, and tumors were excised after reaching a predetermined size. After excision, 30 mice were split into three groups: Controls, NIR-PIT 1 day prior to surgery and NIR-PIT 3 days prior to surgery. The quantity of reactive oxygen species (ROS) in each wound was measured on Postoperative Days 2 and 4, and mice were monitored weekly for 4 weeks for evidence of local tumor recurrence as well as clinical evidence of wound healing complications (eg, dehiscence, infection). The remaining 20 mice (10 controls, 10 treated with NIR-PIT 1 day prior to surgery) were sacrificed on either Postoperative Day 7 or 14, the skin around wounds were excised, and tensile strength was measured with a digital force gauge. There were no significant differences between treatment and control groups with respect to wound ROS levels, wound tensile strength, local tumor recurrence, or postoperative complication rates ($P > .05$). In conclusion, neoadjuvant (pre-operative) NIR-PIT shows no evidence of adverse wound healing effects, and it is likely a safe adjunctive treatment to surgery. Postoperative use of NIR-PIT merits investigation.

KEYWORDS

near-infrared photoimmunotherapy, neoadjuvant, reactive oxygen species, surgery, wound healing

1 | INTRODUCTION

Cancer continues to be a major global health challenge.¹ Near-infrared photoimmunotherapy (NIR-PIT) is a novel cancer therapy that utilized antibody-photoabsorber conjugate

(APC) and near infrared light. NIR-PIT causes cancer-cell selective cytotoxicity with minimal off-target effects and has successfully targeted a diversity of cancers in the preclinical setting.^{2,3} NIR-PIT triggers an intensely immunogenic cell death⁴ that leads to a rapid inflammatory response followed

This is an open access article under the terms of the Creative Commons Attribution License, which permits use, distribution and reproduction in any medium, provided the original work is properly cited.

Published 2020. This article is a U.S. Government work and is in the public domain in the USA. *Cancer Medicine* published by John Wiley & Sons Ltd.

by a cancer antigen-specific immune response. This latter response plays a central role in the treatment's overall efficacy.⁵⁻⁷ NIR-PIT may have a particular role in the neoadjuvant or adjuvant settings of solid tumor surgery, including downstaging or debulking of tumors *prior* to surgery or as a method of removing residual or microscopic tumor(s) immediately *after* surgery from excision sites or large surfaces (eg, peritoneum).⁸⁻¹⁰ In either case, predicting the effect of NIR-PIT on wound healing would be important.

Wound healing is a complex physiologic process that involves overlapping phases of inflammation, proliferation, and tissue remodeling.¹¹ Wound healing is negatively affected by excessive inflammation in both animal models^{12,13} and humans.^{14,15} The immune activation stimulated by NIR-PIT may therefore affect this physiologic process. One quantitative means of measuring this process includes bioluminescence imaging using the chemiluminescent Luminol derivative L-012 (C₁₃H₈CIN₄NaO₂).^{16,17} Luminol is a relatively new means of quantifying reactive oxygen species (ROS) in murine wound models,¹⁸ and differences in wound ROS with vs without NIR-PIT would suggest a potential negative impact on wound healing. Direct measurement of wound tensile strength is another validated method of ascertaining interference in wound healing in murine models.¹⁹ Thus, using these methods, we investigated the effects of perioperative NIR-PIT on postoperative wound healing in a murine model of cancer.

2 | MATERIAL AND METHODS

2.1 | Cell lines and culture

The HER2-positive human gastric cancer cell line, N87GFP-luc, was used for all studies. The cells express both Green Fluorescent Protein (GFP) and Luciferase (Luc). Cells were grown in RPMI 1640 (Life technologies) containing 10% fetal bovine serum (Life Technologies), 0.03% L-glutamine, 100 units mL⁻¹ penicillin and 100 mg mL⁻¹ streptomycin in 5% CO₂ at 37°C.

2.2 | Reagents and APC synthesis

The monoclonal antibody (mAb) used for APC synthesis was Trastuzumab (Herceptin, Genentech), an IgG1 kappa, humanized mAb against HER2, maintained at 4°C in stock solution. The dye was IRDye 700Dx ester (IR700; C₇₄H₉₆N₁₂Na₄O₂₇S₆Si₃, MW: 1954.22), and it was purchased from LI-COR Bioscience. All other chemicals were of reagent grade.

One milligram (6.8 nmol) of Trastuzumab was incubated with 66.8 μg (34.2 nmol) IR700 (5 mmol L⁻¹ in DMSO) in 0.1 mol L⁻¹ Na₂HPO₄ (pH 8.6) at room temperature

for 1 hour. The mixture was subsequently purified with a Sephadex G50 column (PD-10; GE Healthcare). The protein concentrations were confirmed with Coomassie Plus Protein Assay Kit (Pierce Biotechnology) by measuring light absorption at 595 nm (8453 Value System; Agilent Technologies). The concentration of IR700 was measured by absorption with spectroscopy to confirm the average number of fluorophore molecules conjugated to each Trastuzumab molecule. APC solutions were individually diluted with PBS to achieve final concentrations of 500 μg mL⁻¹.

2.3 | NIR-PIT on a mouse tumor model

All in vivo procedures were conducted in compliance with the Guide for the Care and Use of Laboratory Animal Resources (1996), US National Research Council, and approved by the Institutional Animal Care and Use Committee. Female homozygote athymic nude mice aged 6-8 weeks were purchased from Charles River (National Cancer Institute). During treatment, mice were anesthetized with isoflurane. 3 × 10⁶ N87GFP-luc cells were injected subcutaneously in the left flank. In treatment mice, 10-14 days after injection, mice with long-axis tumor diameters between 5 and 9 mm and total tumor volume (as given by the formula 0.5 × length × width × depth) between 50 and 150 mm³ were injected with 100 μg APC through tail vein injection. Twenty-four hours later, NIR laser light (690 ± 5 nm) was administered at a dose of 50 J cm⁻² (Modulight Inc ML7710; Cylindrical Light Diffuser Model: R030). Experimental design after

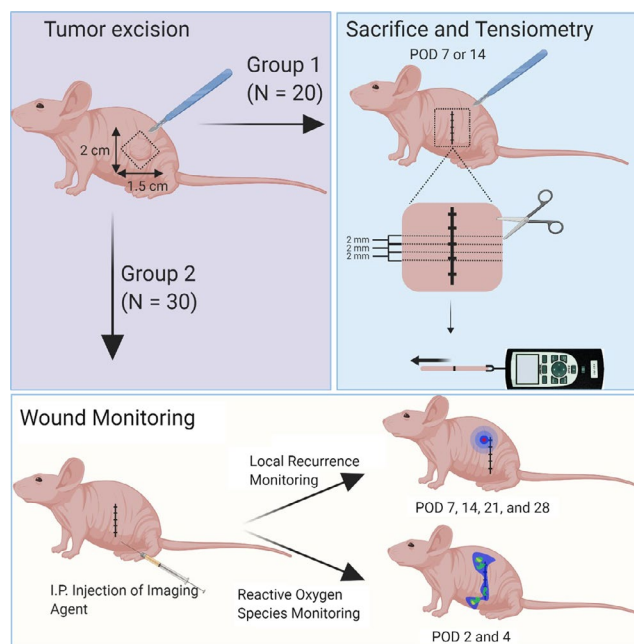


FIGURE 1 Scheme for experimental planning. POD, postoperative date

treatment is illustrated in Figure 1. Briefly, 20 mice were used for tension experiments (see below), 10 treatment mice (NIR 1 day prior to surgery) were evaluated at 7 ($n = 5$) or 14 ($n = 5$) days after surgery, and control mice were divided in the same manner. Thirty mice were monitored for local recurrence, with 10 receiving NIR-PIT 3 days before surgery, 10 1 day before surgery, and 10 controls.

2.4 | Survival surgery

2.4.1 | Surgery

Tumors were surgically excised at either Day 1 or 3 post-NIR-PIT in the experimental group, or at the time the tumor reached the same size for controls. Five minutes before incision, mice were simultaneously administered three medications intraperitoneally: 5 mg kg⁻¹ of Xylazine and 2 mg kg⁻¹ of Ketamine for intraoperative sedation and anesthesia, and 0.25 mg kg⁻¹ Buprenorphine for postoperative pain control. Immediately prior to incision, tumor size was recorded and the left trunk, from foreleg to hindleg, was scrubbed with three rounds of alternating Betadine solution (10% Povidone Iodine, Purdue Pharma) and reagent grade Isopropyl Alcohol (Sigma Aldrich). A 2 × 1.5 cm excisional square was then marked around the tumor, and the skin and underlying tumor were excised. Intraoperative *in vivo* fluorescence imaging was then performed with the Maestro In Vivo Fluorescence Imager (Cri, Woburn, MA, USA) using a 445-490 nm band pass excitation filter with a long pass emission filter over 515 nm to confirm complete tumor excision. Topical Bupivacaine drops were added to the wound up to a maximum of 8 mg kg⁻¹ for intraoperative pain control if there was any evidence of pain (eg, twitching or increased respiratory rate). The excised GFP-positive tumor was included in the images as a positive control. Mice were excluded if complete excision could not be verified after three attempts ($n = 1$) or if there was peritoneal invasion ($n = 4$). Wounds were closed with three to four simple interrupted sutures using 4-0 nylon sutures (UNIFY). Immediately after wound closure, 4 mg kg⁻¹ Ketoprofen was subcutaneously injected for further control of postoperative pain. Surgical instruments were autoclaved in 20-minute cycles (AMSCO Century, Steris) at the beginning of each surgery day and were sterilized in between surgeries with a glass bead sterilizer (Germinator 500; Cellpoint Scientific).

2.4.2 | Postoperative care

Mice were monitored daily for pain in the first postoperative week and every 2 days thereafter. In the first

intraoperative week, mice were housed individually and fitted with Elizabethan Collars (E-Collars) (Kent Scientific Corporation) to prevent biting of sutures. To prevent ocular infections, E-Collars were removed for 5 minutes under direct observation on the first and third days after surgery to allow for mouse self-grooming. After the first week, E-collars and any remaining sutures were removed. Mice were housed together after the second week.

2.5 | Postoperative wound monitoring

2.5.1 | Reactive oxygen species monitoring

In the wound monitoring group (group 2), ROS monitoring was performed on both experimental and control mice on Postoperative Day 2 and 4. The bioluminescence of the ROS in each wound was imaged and quantified using a photon counting imaging system (PhotonIMAGER OPTIMA; Biospace Lab). The Luminol derivative L-012 (FUJIFILM Wako Pure Chemical Corporation) was administered intraperitoneally (0.5 mg 20 g⁻¹) 50 minutes prior to imaging. Imaging duration was 2 minutes. Regions of Interest (ROI) were placed over the wounds, and counts of Relative Light Units were analyzed using M3 Vision Software (Biospace Lab).

2.5.2 | Local recurrence monitoring and postoperative complication monitoring

In the wound monitoring group, mice were also monitored for local recurrence on Postoperative Days 7, 14, 21, and 28. Luciferin was intraperitoneally administered (15 mg mL⁻¹, 200 μL) and bioluminescence (BLI) images were acquired 15 minutes later using a BLI camera (PhotonIMAGER Optima). Daily monitoring for postoperative complications revealed no instances of wound dehiscence or local or systemic infection.

2.5.3 | Wound tensile strength measurements

In Group 2, experimental and control mice were euthanized at either Postoperative Day 7 or Day 14, and a rectangle piece of skin encompassing the entire wound was excised and cut into multiple 2-millimeter (mm)-wide strips. The most peripheral strips (those from the dorsal and ventral wound ends) were not used. For each mouse, the tensile strength of three strips was measured by applying manual tension orthogonal to the direction of incision with opposite end of the strip clamped by a handheld digital force gauge (DST-1A; IMADA Inc).

2.5.4 | Confirmatory imaging

Treatment groups of mice were imaged with IR700 fluorescence before and after laser therapy using an in vivo fluorescence imager (Pearl Imager, LI-COR Bioscience) to confirm treatment efficacy. Complete resection of GFP positive tumors was confirmed with Maestro Imaging (see Section 2.4.1 above) and Local recurrence was monitored with a BLI camera (see Section 2.5.2 above).

2.6 | Statistical analysis

All statistical analyses were performed with GraphPad Prism (GraphPad Software). *P* values <.05 were considered significant.

3 | RESULTS

3.1 | Local recurrence rates and postoperative complications

There was no significant difference in recurrence rates, with a 10% local recurrence in each treatment group ($n = 1$ for each) and a 20% local recurrence rate in the control group ($n = 2$). There were no instances of thermal injury in the treatment groups, and no instances of wound infection or dehiscence in any mice (Table 1).

3.2 | Reactive oxygen species

Mean photon counts in ROIs placed directly over the wounds were not significantly different between experimental groups ($P > .05$ for both postoperative date (POD) 2 and 4; one-way analysis of variance (ANOVA), Figure 2A). Given that genetic variability among mice may cause variability in luminescence, the ratio of POD4 to POD2 photon counts was also measured. This ratio was not significantly different between treatment groups ($P = .37$; one-way ANOVA, Figure 2B; representative images in Figure 3).

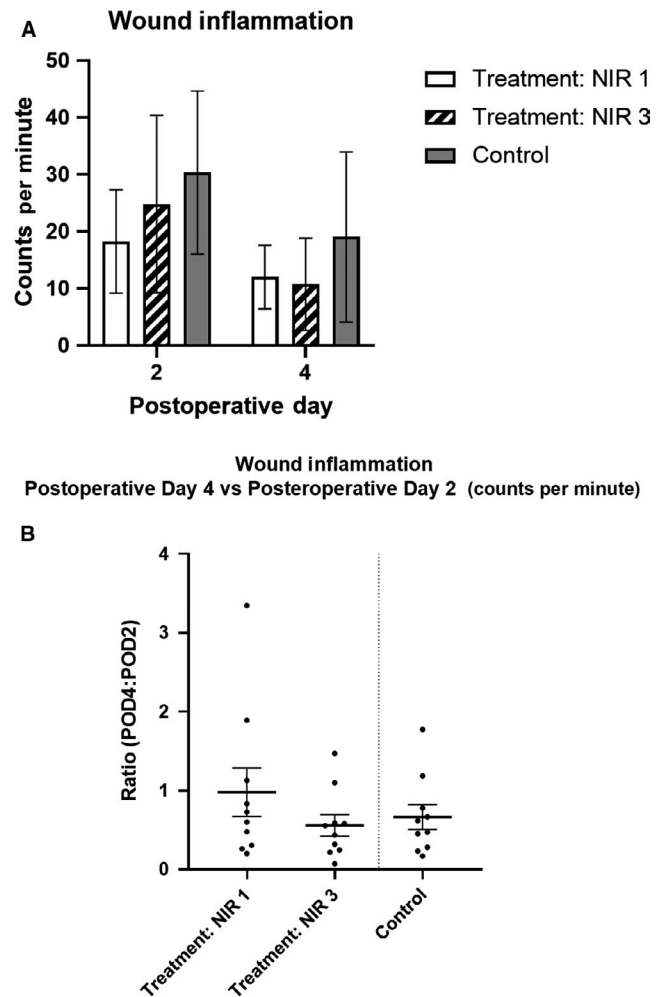


FIGURE 2 Inflammation at the wound. A, Mean wound inflammation was not significantly different between experimental groups ($P > .05$ for both POD 2 and 4; one-way ANOVA). B, Ratio of POD4 to POD2 inflammation was not significantly different between treatment groups ($P = .37$; one-way ANOVA). Error bars represent SEMs. Treatment NIR 1 and 3 = surgery performed day one and three post-NIR-PIT, respectively. Inflammation measured via photon imaging of reactive oxygen species 50 min after intraperitoneal administration of $0.5 \text{ g } 20 \text{ g}^{-1}$ dose of L-012. POD, postoperative date

3.3 | Wound tensile strength

Mean wound tension was not significantly different between mice in a given experimental group ($P > .05$ for each group

TABLE 1 Monitoring for local recurrence and postoperative complications

	Treatment: NIR 1 (N = 10)	Treatment: NIR 3 (N = 10)	Control (N = 10)
Local recurrence	10% (1)	10% (1)	20% (2)
Wound dehiscence	0 (0)	0 (0)	0 (0)
Wound infection	0 (0)	0 (0)	0 (0)
Thermal injury	0 (0)	0 (0)	Not applicable

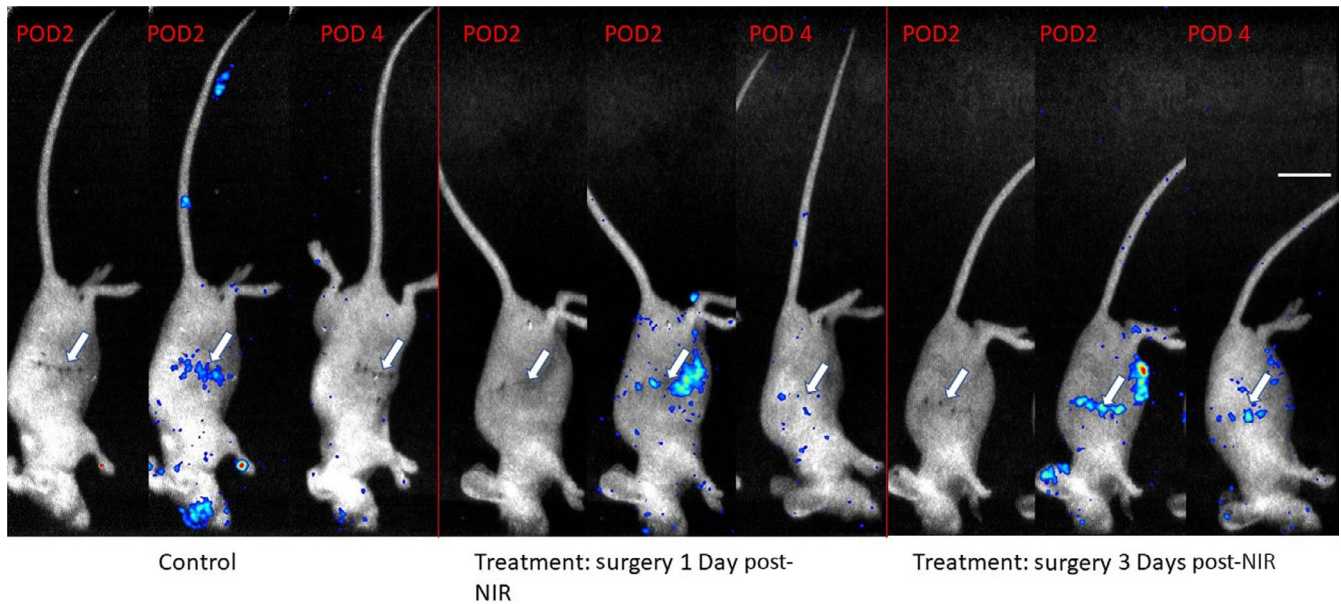


FIGURE 3 Singlet oxygen production at the wound. Representative mouse from each group, shown at Postoperative Day 2 (POD2) with white light images (to visualize the wound), Postoperative Day 2 with ROS signal included, and Postoperative Day 4 (POD4) with ROS signal included, respectively. Signal represents counts. Counts decrease significantly between POD 2 and POD 4. Reactive Oxygen Species elicited via intraperitoneal injection of L-012 ($0.5 \text{ mg } 20 \text{ g}^{-1}$) 50 min prior to imaging. Imaging window = $0.05\text{--}0.50 \times 10^{-3}$ counts for images in which ROS signal is included. In some mice, there is observable inflammation near the eyes (post-operative inflammation secondary to Elizabethan collar usage, preventing self-grooming), ears (location of hole-punching for identification), and site of peritoneal injections. Arrows indicate where the tumors were located. Scale bar represents 1 cm

using one-way ANOVA, Figure 4A), demonstrating little inter-mouse variability in wound strength. Mean tension in the control group vs treatment groups showed nonsignificant differences at their respective timepoints ($P > .05$ for both Postoperative Day 7 and 14; unpaired t test with Welch's correction; Figure 4B).

3.4 | Confirmatory imaging

In vivo fluorescence imaging of IR700 before NIR light irradiation confirmed localization of APC in tumor. Missing IR700 fluorescence after NIR light irradiation confirmed successful photochemical reaction to NIR light (Figure 5A). GFP fluorescent imaging confirmed complete tumor resection (Figure 5B). Bioluminescence imaging showed local recurrence of luciferase expressing tumor (Figure 5C).

4 | DISCUSSION

In this study, we show that in murine models of subcutaneously grafted tumors, NIR-PIT either 1 or 3 days prior to excision did not affect the level of wound inflammation or strength of wounds after surgery. These results provide evidence that NIR-PIT does not interfere with postsurgical healing and therefore, could be safely used in a perioperative clinical setting. An example of such use might be NIR-PIT

to de-bulk tumors deemed too large for initial resection or reduce tumor volume in palliative treatments, without risk of adverse wound healing effects.

We used several measures of wound healing integrity to determine the effects of NIR-PIT. A central component of wound monitoring was serial bioluminescence imaging to detect inflammation by ROS. In wound healing, basal levels of ROS are necessary to recruit lymphoid cells and promote angiogenesis and wound disinfection, though excessive ROS can cause oxidative stress at levels that inhibit cellular migration and fibroblast proliferation and promote cellular necrosis.²⁰ Importantly, ROS are not simply surrogates of inflammation, but play a direct role in the repair and remodeling of wounds.²¹ In this study, ROS levels trended lower in the treatment group, but no significant difference between treatment and control groups on Postoperative Days 2 and 4 ($P = .37$) was observed.

Wound integrity was also measured with tensile strength measurement, which has a well-established role for the evaluation of both human and animal wound healing.^{22,23} The tensile strength data in this study provided important evidence of unimpaired wound healing. Wound tension at Postoperative Day 7 and 14 was identical between treatment and control mice, indicating that wounds were likely healing at similar rates between groups.

Inflammation at the wound site is also known to promote tumorigenesis and worsen recurrence rates.^{24–26}

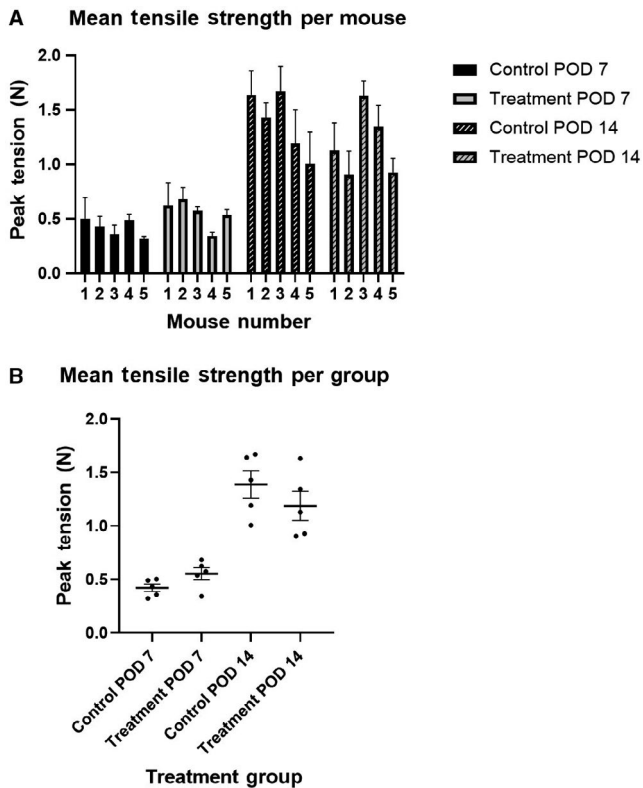


FIGURE 4 Wound tensile strength. A, Mean wound tension was not significantly different between mice in a given group ($P > .05$ for each group using one-way ANOVA). B, Mean tension in control group vs treatment groups showed nonsignificant differences at their respective timepoints (mean tension POD 7: control = 0.42, treatment = 0.55, $P = .096$. POD 14: control = 1.39, Treatment = 1.19, $P = .314$; unpaired t test with Welch's correction). POD 7 and 14 = wound tension measured on Postoperative Days 7 and 14, respectively. $N = 5$ mice per group. $N = 3$ measurements per mouse, using three 2-mm-wide segments of skin tissue included wound. Tension applied orthogonal to direction of incision and suture. Error bars represent SEMs

Wounds were therefore monitored for local recurrence over the course of 4 weeks using previously validated bioluminescence imaging techniques,²⁷ and no significant difference in rates of recurrence were found for the treatment and control groups.

This study explored the use of NIR-PIT in the preoperative setting, but postoperative use is another important question to be investigated. There is some evidence that infrared light using parameters similar to those of this study (685 ± 5 nm, 50 J cm^{-2}) is safe and perhaps beneficial for wound healing. Pinheiro et al reported that a 40 J cm^{-2} dose of 685 nm light in excisional wound rat models showed histologic features of wound healing equal to that of controls, and in the 20 J cm^{-2} group they reported histologic features suggestive of improved wound healing.²⁸ In incisional rat models, Suzuki and Takakuda also report increased tensile strength and increased collagen deposition 7 days after wounding when wounds were treated with 660 nm light 24 hours after surgery with doses as small as 1 and 5 J cm^{-2} , though not at 10 J cm^{-2} .²⁹ Finally, Lackjavoca et al report improved wound healing with 670 nm 5 J cm^{-2} dosing of excisional wound rat models.³⁰ Thus, the potential role of NIR-PIT as a postsurgical adjuvant, with light administered even directly on fresh wounds, merits investigation.

5 | LIMITATIONS AND CONSIDERATIONS

The differences between mouse and human skin are well documented.³¹ Additionally, although athymic nude mice were chosen because their skin is not confounded by the effects of hair growth on wound healing,^{32,33} the lack of mature T cells

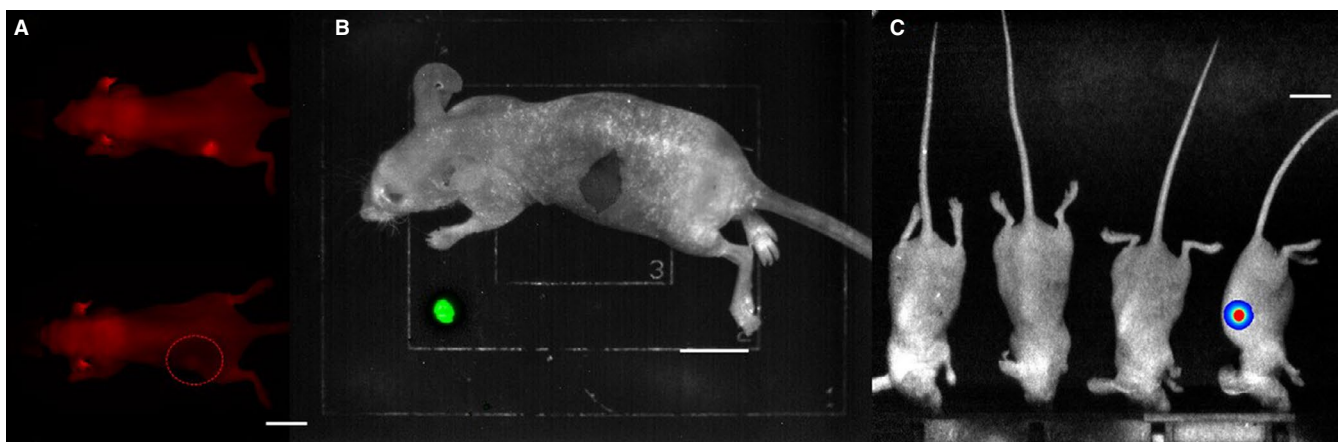


FIGURE 5 Definition of imaging procedures. A, Confirmation of antibody-photoabsorber conjugate (APC) localization to the tumor and photochemical reaction to infrared light administration. Images taken immediately before (top) and after (lower) NIR light exposure, respectively. APC was administered 24 h prior to laser therapy. B, Intraoperative confirmation of complete tumor excision using in vivo fluorescence imaging of GFP-positive tumors. Excised tumor included as positive control. C, Representative batch of control mice on Postoperative Day 7. Local recurrence detected in the rightmost mouse. Recurrence of Luciferase positive tumors is detected by intraperitoneal injection of Luciferin 15 min prior to imaging. Scale bars represent 1 cm

may affect results, as the role of T lymphocytes in wound healing has recently begun to be elucidated.^{34,35} Finally, suture technique (eg, simple interrupted vs running suture) affects wound tensile strength in murine models and should be carefully considered in study designs.³⁶ In conclusion, in murine cancer models, neoadjuvant administration of NIR-PIT shows no evidence of adverse effects on wound healing. These results support the premise that NIR-PIT is likely to be a safe adjunct to surgical treatment of solid tumors, and future investigations of NIR-PIT in the perioperative setting are merited.

ACKNOWLEDGMENTS

This research was supported by the Intramural Research Program of the NIH, National Cancer Institute, Center for Cancer Research (ZIA BC 011513). FI was also supported with a grant from National Center for Global Health and Medicine Research Institute, Tokyo, Japan. For AR, this research was made possible through the NIH Medical Research Scholars Program, a public-private partnership supported jointly by the NIH and contributions to the Foundation for the NIH.

CONFLICTS OF INTEREST

The authors have no conflicts of interest to be reported.

AUTHORS' CONTRIBUTION


AR, FI, TK, and RO mainly designed and conducted experiments, performed analysis and wrote the manuscript; HW, and AF performed analysis; PLC wrote and edited the manuscript and supervised the project; and HK planned and initiated the project, designed and conducted experiments, wrote and edited the manuscript, and supervised the entire project.

DATA AVAILABILITY STATEMENT

The data that support the findings of this study are available from the corresponding author upon reasonable request.

ORCID

Fuyuki Inagaki  <https://orcid.org/0000-0002-9953-3805>

Hisataka Kobayashi  <https://orcid.org/0000-0003-1019-4112>

REFERENCES

- Siegel RL, Miller KD, Jemal A. Cancer statistics, 2019. *CA Cancer J Clin*. 2019;69(1):7.
- Makoto M, Mikako O, Nobuyuki K, Lauren TR, Peter LC, Hisataka K. Cancer cell-selective in vivo near infrared photoimmunotherapy targeting specific membrane molecules. *Nat Med*. 2011;17(12):1685.
- Kobayashi H, Choyke PL. Near-infrared photoimmunotherapy of cancer. *Acc Chem Res*. 2019;52(8):2332.
- Ogawa M, Tomita Y, Nakamura Y, et al. Immunogenic cancer cell death selectively induced by near infrared photoimmunotherapy initiates host tumor immunity. *Oncotarget*. 2017;8(6):10425.
- Kiss B, Van Den Berg NS, Ertsey R, et al. CD47-targeted near-infrared photoimmunotherapy for human bladder cancer. *Clin Cancer Res*. 2019;25(12):3561.
- Nagaya T, Friedman J, Maruoka Y, et al. Host immunity following near-infrared photoimmunotherapy is enhanced with PD-1 checkpoint blockade to eradicate established antigenic tumors. *Cancer Immunol Res*. 2019;7(3):401.
- Maruoka Y, Furusawa A, Okada R, et al. Combined CD44- and CD25-targeted near-infrared photoimmunotherapy selectively kills cancer and regulatory T cells in syngeneic mouse cancer models. *Cancer Immunology Research*. 2020;8(3):345-355.
- Nagaya T, Okuyama S, Ogata F, Maruoka Y, Choyke P, Kobayashi H. Near infrared photoimmunotherapy using a fiber optic diffuser for treating peritoneal gastric cancer dissemination. *Gastric Cancer*. 2019;22(3):463.
- Photoimmunotherapy lowers recurrence after pancreatic cancer surgery in orthotopic nude mouse models (Report). *J Surg Res*. 2015;197(1):5.
- Moore LS, Boer E, Warram JM, et al. Photoimmunotherapy of residual disease after incomplete surgical resection in head and neck cancer models. *Cancer Med*. 2016;5(7):1526.
- Li J, Chen J, Kirsner R. Pathophysiology of acute wound healing. *Clin Dermatol*. 2007;25(1):9.
- Qian LW, Fourcaudot AB, Yamane K, You T, Chan RK, Leung KP. Exacerbated and prolonged inflammation impairs wound healing and increases scarring. *Wound Repair Regen*. 2016;24(1):26.
- Bettinger DA, Pellicane JV, Tarry WC, et al. The role of inflammatory cytokines in wound healing: accelerated healing in endotoxin-resistant mice. *J Trauma*. 1994;36(6):810.
- Menke NB, Ward KR, Witten TM, Bonchev DG, Diegelmann RF. Impaired wound healing. *Clin Dermatol*. 2007;25(1):19.
- Nwomeh BC, Liang HX, Diegelmann RF, Cohen IK, Yager DR. Dynamics of the matrix metalloproteinases MMP-1 and MMP-8 in acute open human dermal wounds. *Wound Repair Regen*. 1998;6(2):127.
- Liu WF, Ma M, Bratlie KM, Dang TT, Langer R, Anderson DG. Real-time in vivo detection of biomaterial-induced reactive oxygen species. *Biomaterials*. 2011;32(7):1796.
- Zielonka J, Lambeth JD, Kalyanaraman B. On the use of L-012, a luminol-based chemiluminescent probe, for detecting superoxide and identifying inhibitors of NADPH oxidase: a reevaluation (Report). *Free Radic Biol Med*. 2013;65:1310.
- Rabbani PS, Abdou SA, Sultan DL, Kwong J, Duckworth A, Ceradini DJ. In vivo imaging of reactive oxygen species in a murine wound model. *J Vis Exp*. 2018;2018(141). <https://doi.org/10.3791/58450>
- Bellare A, Epperly MW, Greenberger JS, Fisher R, Glowacki J. Development of tensile strength methodology for murine skin wound healing. *MethodsX*. 2018;5:337.
- Dunnill C, Patton T, Brennan J, et al. Reactive oxygen species (ROS) and wound healing: the functional role of ROS and emerging ROS-modulating technologies for augmentation of the healing process. *Int Wound J*. 2017;14(1):89.
- Bryan N, Ahswain H, Smart N, Bayon Y, Wohlert S, Hunt JA. Reactive oxygen species (ROS) – a family of fate deciding molecules pivotal in constructive inflammation and wound healing. *Eur Cells Materials*. 2012;24:249.
- Lindstedt E, Sandblom P. Wound healing in man: tensile strength of healing wounds in some patient groups. *Ann Surg*. 1975;181(6):842.

23. Gottrup F, Ågren MS, Karlsmark T. Models for use in wound healing research: a survey focusing on in vitro and in vivo adult soft tissue. *Wound Repair Regen.* 2000;8(2):83.
24. Abramovitch R, Marikovsky M, Meir G, Neeman M. Stimulation of tumour growth by wound-derived growth factors. *Br J Cancer.* 1999;79(9-10):1392.
25. Martins-Green M, Boudreau N, Bissell MJ. Inflammation is responsible for the development of wound-induced tumors in chickens infected with Rous sarcoma virus. *Can Res.* 1994;54(16):4334.
26. Ceelen W, Pattyn P, Mareel M. Surgery, wound healing, and metastasis: recent insights and clinical implications. *Crit Rev Oncol Hematol.* 2014;89(1):16.
27. Maruoka Y, Nagaya T, Nakamura Y, et al. Evaluation of early therapeutic effects after near-infrared photoimmunotherapy (NIR-PIT) using luciferase-luciferin photon-counting and fluorescence imaging. *Mol Pharm.* 2017;14(12):4628.
28. Pinheiro ALB, Pozza DH, Oliveira MGD, Weissmann R, Ramalho LMP. Polarized light (400–2000 nm) and non-ablative laser (685 nm): a description of the wound healing process using immunohistochemical analysis. *Photomed Laser Sur.* 2005;23(5):485.
29. Suzuki R, Takakuda K. Wound healing efficacy of a 660-nm diode laser in a rat incisional wound model. *Lasers Med Sci.* 2016;31(8):1683.
30. Lacjaková K, Bobrov N, Poláková M, et al. Effects of equal daily doses delivered by different power densities of low-level laser therapy at 670 nm on open skin wound healing in normal and corticosteroid-treated rats: a brief report. *Lasers Med Sci.* 2010;25(5):761.
31. Wong VW, Sorkin M, Glotzbach JP, Longaker MT, Gurtner GC. Surgical approaches to create murine models of human wound healing. *J Biomed Biotechnol.* 2011;2011:1-8.
32. Müller-Röver S, Foitzik K, Paus R, et al. A comprehensive guide for the accurate classification of murine hair follicles in distinct hair cycle stages. *J Invest Dermatol.* 2001;117(1):3.
33. David MA, Jennifer EK, Helen AT, Ralf P, Matthew JH. Exploring the “hair growth-wound healing connection”: anagen phase promotes wound re-epithelialization. *J Invest Dermatol.* 2010;131(2):518.
34. Schäffer M, Barbul A. Lymphocyte function in wound healing and following injury. *Br J Surg.* 1998;85(4):444.
35. Park JE, Barbul A. Understanding the role of immune regulation in wound healing. *Am J Surg.* 2004;187(5):S11.
36. Gál P, Toporcer T, Vidinský B, Hudák R, Živčák J, Sabo J. Simple interrupted percutaneous suture versus intradermal running suture for wound tensile strength measurement in rats: a technical note. *Eur Surg Res.* 2009;43(1):61-65.

How to cite this article: Rosenberg A, Inagaki F, Kato T, et al. Wound healing after excision of subcutaneous tumors treated with near-infrared photoimmunotherapy. *Cancer Med.* 2020;9:5932–5939. <https://doi.org/10.1002/cam4.3247>